



Contents lists available at ScienceDirect

Journal of Interventional Medicine

journal homepage: www.keaipublishing.com/cn/journals/journal-of-interventional-medicine/

Feasibility of CT-CT fusion imaging for evaluation of the cryoablation margins in visible hepatocellular carcinoma on unenhanced CT images: Initial experience

Chao Chen, Yaohui Wang, Guodong Li, Lichao Xu, Ying Wang, Haozhe Huang, Biao Wang, Wentao Li^{*}, Xinhong He^{**}

Department of Interventional Radiology, Fudan University Shanghai Cancer Center, Shanghai, 200032, China

ARTICLE INFO

Keywords:

Computed tomography
Fusion
Hepatocellular carcinoma
Cryoablation
Ablative margin

ABSTRACT

Objective: To demonstrate the feasibility of CT-CT fusion imaging for assessment of the cryoablation margins in visible hepatocellular carcinoma (HCC) on unenhanced CT images.

Methods: This retrospective study analyzed 14 patients with 14 HCC lesions treated with CT-guided cryoablation. Nine lesions in nine patients who developed local tumor progression (LTP) during the follow-up period of at least 8 months were reviewed. The unenhanced CT data were used to retrospectively create fusion images of the intraoperative CT images on a workstation. The minimal ablative margin (MAM) was assessed on the fusion images. The concordance between the site of LTP and the MAM area was also assessed.

Results: Eight of the nine lesions with LTP were in the subcapsular region of the liver. Seven of the nine cases were treated by cryoablation combined with transcatheter arterial chemoembolization. The median time required to fuse the images for the nine lesions was 5:17 min (range, 5:04–7:37 min). The site of LTP relative to the HCC lesion was cranio-caudal in nine, dorsoventral in six, and lateral in seven lesions. In all lesions, the site of LTP was congruent with the MAM area.

Conclusions: CT-CT fusion imaging enables a real-time intraoperative treatment evaluation for HCC lesions visible on unenhanced CT images. Fused imaging evaluation has proved to be an accurate and useful tool for assessment of the cryoablation margins.

Introduction

Hepatocellular carcinoma (HCC) is the most common type of liver cancer and the second leading cause of cancer-related deaths, worldwide.¹ Nearly half of the newly diagnosed HCC cases occur in China.² Local tumor ablative techniques, such as cryoablation and radiofrequency ablation (RFA), may offer alternative treatment options for those with an unresectable HCC. Although RFA is the most commonly used ablation modality, the use of cryoablation has been increasing.³ Because of a different tumor ablation mechanism, cryoablation has potential advantages over RFA, including the ability to visualize the ice ball,^{4,5} activation of a cryo-immunologic response in cancer,⁶ lack of severe damage to the large blood vessels,⁷ and less severe pain.^{8,9}

Imaging is commonly used to monitor and assess the results of thermal ablation procedures. The minimal ablative margin (MAM) in RFA is

assessed by comparing the axial images of CT, MRI, or contrast-enhanced ultrasound obtained before and after RFA using a side-by-side approach.^{10–12} However, it is quite difficult to visually grasp the positional relation of the tumor and the ablation zone, and accurately measure the MAM. Recently, the development of new image fusion techniques has made it possible to accurately assess the MAM and the therapeutic responses to RFA for HCC.^{13–15} To the best of our knowledge, no prior study has evaluated the treatment effect of cryoablation using fusion imaging, particularly in the liver.

For pre- and post-treatment fusion imaging, there are some challenges, such as the deformation of the liver because of the difference in the patient's position¹⁶ and the variations in the slice thickness of the pre- and post-treatment CT images.¹⁴ To overcome these limitations and take advantage of the clear ablation zone of cryoablation, we used the intraoperative CT images to create the fusion images. Therefore, the purpose

* Corresponding author.

** Corresponding author.

E-mail addresses: wentaoli@fudan.edu.cn (W. Li), hxhdoct@hotmail.com (X. He).

<https://doi.org/10.1016/j.jimed.2019.09.003>

Available online 9 September 2019

2096-3602/Copyright © 2019 Shanghai Journal of Interventional Medicine Press. Production and hosting by Elsevier B.V. on behalf of KeAi. This is an open access

article under the CC BY-NC-ND license (<http://creativecommons.org/licenses/by-nc-nd/4.0/>).

of our study was to demonstrate the effectiveness of CT-CT fusion imaging for the evaluation of the treatment effect of cryoablation in patients with HCC.

Materials and methods

Patients

Our Institutional Review Board approved this retrospective study and the need for informed consent was waived. From August 2014 to September 2015, 14 patients with a total of 14 HCC lesions underwent cryoablation. Six of the 14 HCC lesions were confirmed by histopathologic analysis, and the remaining tumors were confirmed as HCC based on the clinical criteria outlined by the American Association for the Study of Liver Diseases.¹⁷ Five tumors were excluded from the analysis for the following reasons: lack of pre- or post-cryoablation contrast-enhanced CT or MRI taken within 1 month ($n = 2$), non-apparent tumors on the unenhanced CT images ($n = 1$), a follow-up period of less than 8 months after cryoablation ($n = 1$), and obvious residual lesions on the contrast-enhanced CT or MRI images at 1 month after cryoablation ($n = 1$). The remaining nine tumors in nine patients (seven men and two women; age range, 53–70 years; mean age, 62.3 years) were finally chosen for this study based on the following inclusion criteria: availability of contrast-enhanced CT or MRI images performed 1 month before the procedure and availability of follow-up CT or MRI images presenting local tumor progression (LTP). In the present study, HCC with LTP was defined as regrowth of the tumor inside or adjacent to the successfully treated HCC nodules after cryoablation that appeared as a hyper-enhancing area in the arterial phase followed by wash-out in the portal/delayed phase on either dynamic CT or MRI.^{18,19}

Study protocol

The protocol comprised the contrast-enhanced CT or MRI scans taken within 1 month before cryoablation, the cryoablation procedure itself, fusion imaging using the initial intraoperative CT image and the intraoperative CT image at the end of cryoablation, assessment of the MAM, follow-up period of more than 8 months, and assessment of the LTP. Finally, the concordance between the site of LTP and the MAM area was assessed.

Percutaneous cryoablation procedure

Cryoablation was performed under local anesthesia on an inpatient basis by physicians with more than 5 years of experience. Before the procedure, 10 mg diazepam was administered by intramuscular injection as basal sedation, supplemented with 5 mg analgesic morphine as required. The patients underwent continuous pulse oximetry and electrocardiography. A 64-slice spiral CT (120 kV, 250 mA, and 3-mm thickness; Philips Healthcare, Andover, MA, USA) was used for imaging guidance, localization, and intraoperative real-time monitoring of the ablation procedures to avoid injury to the surrounding critical structures.

A tabletop argon gas-based cryoablation apparatus (Precise Cryoablation System; Galil Medical, Yokneam, Israel) with 17-gauge cryoprobes was used to perform the procedure. The cryoprobes were placed into the lesion within 1.5 cm of the tumor edge, but with less than 2 cm intervals between the probes.²⁰ The number and type of probes used depended on the preoperative tumor volume in order to ensure producing precise ice balls that encompassed the target tumor. After the cryoprobes had been placed, the cryosurgery system was initiated to begin rapid freezing. A double freeze-thaw cycle (15 min/time: freeze for 10 min and thaw for 5 min) was performed according to the standard protocol. An additional cycle was necessary if the ablation zone was not satisfactory.

Image fusion procedure

If the contrast-enhanced CT or MR images at 1 month after cryoablation showed that the lesion had been completely ablated, image fusion was further performed. An abdominal radiologist with 8 years of experience, who was blinded to the clinical history of the patients prior to the ablation and the information of LTP, performed the fusion imaging. The intraoperative CT images were sent to a workstation (Advantage Workstation Volume share 5; GE Healthcare Japan) equipped with the necessary software (Integrated Registration; GE Healthcare Japan), and fused images of the initial intraoperative CT images (CT images before cryoneedle insertion) and the intraoperative CT images at the end of cryoablation (cryoneedle still in tumor) were created (Figs. 1 and 2). Automatic image registration was performed by aligning two overlaid CT images with six parameters, namely, translation and rotation in three reformed planes (axial, coronal, and sagittal), in order to maximize the alignment of the tumor and the ablation zone in the images. Blood vessels, cysts, scars, or the hepatic contour near the tumor were used as landmarks for fine adjustments. Landmarks closer to the tumor were preferred as they allowed for a more accurate image fusion.¹⁴ The time required to fuse the images was recorded.

Assessment of the MAM

The fused images were simultaneously interpreted by two abdominal imaging radiologists with 8 and 10 years of experience, respectively, and consensus was obtained by discussion. When they adjudged that the fused images were appropriate for measurement of the MAM, which is the shortest distance between the tumor boundaries and the ablation zone on axial images, they measured the MAM. The relationships of the MAM to the ablative margins were divided into six directions (cranial, caudal, ventral, dorsal, right, and left) by three reformed planes (axial, coronal, and axial).

Follow-up procedure

For evaluation of the therapeutic response, a follow-up contrast-enhanced CT or MRI scan was performed for all patients 1 month after the cryoablation procedure. If the cryoablation was considered to be technically effective, a follow-up contrast-enhanced CT or MRI scan was repeated every 2 months thereafter in the first year. The follow-up interval was then extended to every 3 months after the first year. The site of LTP on the contrast-enhanced CT or MR images was recorded. The concordance between the site of LTP and the MAM area was assessed.

Results

There were no treatment-related deaths or severe complications in any of the patients. The patients' clinical characteristics are presented in Table 1. Eight of the nine LTPs occurred in the subcapsular region of the liver. Seven of the nine cases were treated by cryoablation combined with transcatheter arterial chemoembolization (TACE) (see Table 2).

The median time required to fuse the images was 5:17 min (range, 5:04–7:37 min). The site of LTP relative to the HCC lesion was cranio-caudal in nine, dorsoventral in six, and lateral in seven lesions. In all lesions, the site of LTP was congruent with the MAM area. The mean time to LTP for all nine lesions was 5 months (range, 2–35 months), whereas the median time to LTP for the seven lesions treated with cryoablation combined with TACE was 7 months (range, 2–35 months).

Discussion

In all cases of LTP, the contrast-enhanced CT or MR images at 1 month after cryoablation showed that the lesion had been completely ablated. However, in all cases, the fused images revealed the cryoablation to be insufficient. The site of LTP was congruent with the MAM area.

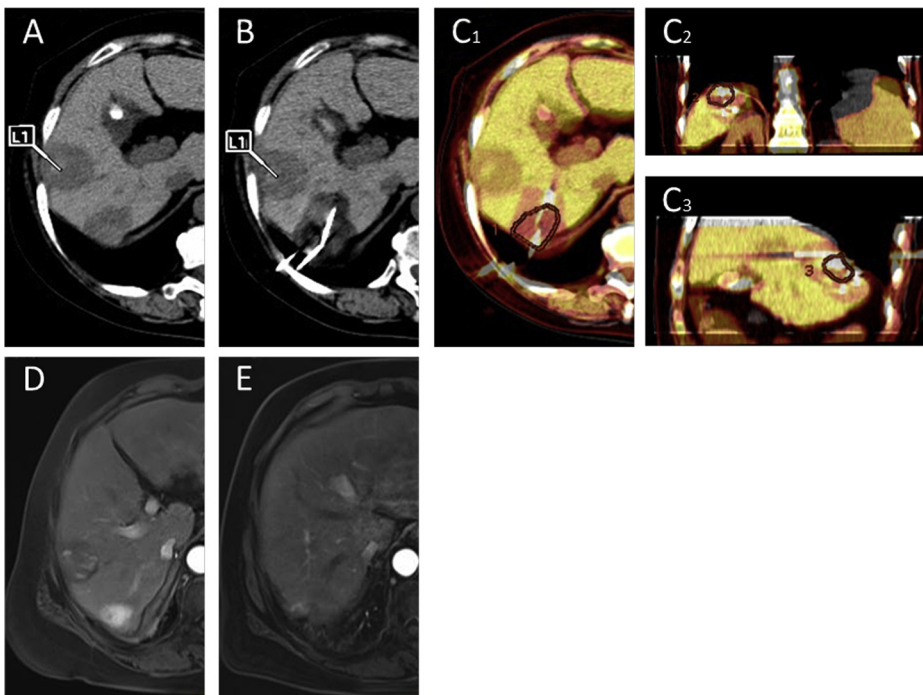


Fig. 1. A 69-year-old woman with visible HCC who was treated with percutaneous cryoablation.

A. A tumor measuring 3.2 cm is noted in Segment 6 on the unenhanced CT image with a low-density area before cryoneedle insertion.

B. An intraoperative CT image at the end of cryoablation (cryoneedle still in tumor) shows a clear ablation zone. The cysts present on both the pre- and post-cryoablation images were manually chosen as landmarks for creating the fused images.

C. A fused image was created after an automatic rigid registration combined with manual correction. The minimal ablative margin (MAM) is to the left (C1), cranial (C2), and dorsal (C3) of the ablation.

D. A contrast-enhanced MR image obtained before cryoablation shows a hypervascular tumor in Segment 6.

E. A contrast-enhanced MR image obtained 18 months after cryoablation shows LTP appearing to the left, cranial, and dorsal of the ablation.

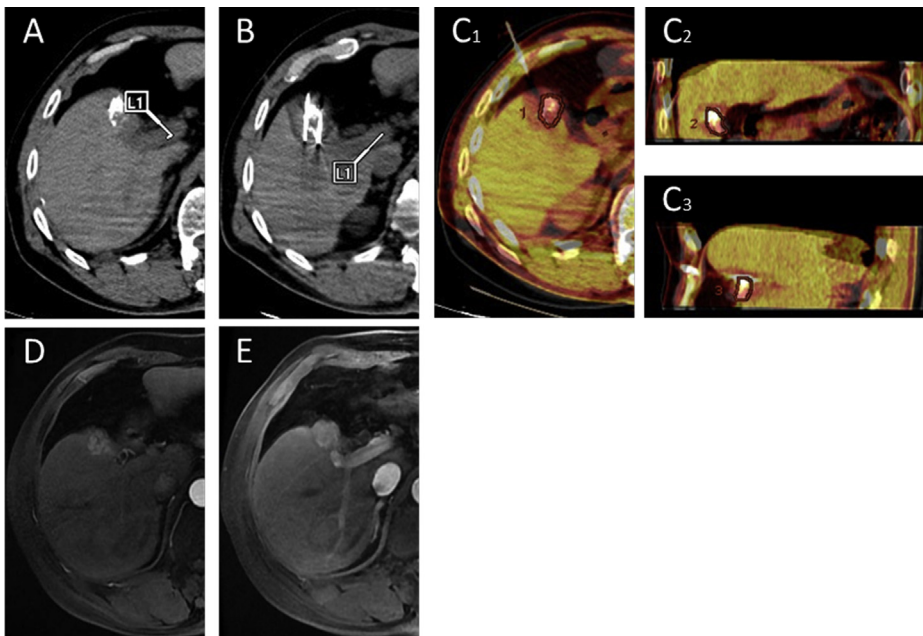


Fig. 2. A 64-year-old man with hepatocellular carcinoma (HCC) who was treated with percutaneous cryoablation.

A. A tumor measuring 2.6 cm is noted in Segment 5 on the unenhanced CT image with lipiodol deposition before cryoneedle insertion.

B. An intraoperative CT image at the end of cryoablation (cryoneedle still in tumor) shows a clear ablation zone and deformation of the lipiodol deposition. Blood vessels present on both the pre- and post-cryoablation images were manually chosen as landmarks for creating the fused images.

C. A fused image was created after an automatic rigid registration combined with manual correction. The minimal ablative margin (MAM) is to the right (C1) and caudal (C2,3) of the ablation.

D. A contrast-enhanced MR image obtained before cryoablation shows a hypervascular tumor in Segment 5.

E. A contrast-enhanced MR image obtained 3 months after cryoablation shows local tumor progression (LTP) appearing to the right and caudal of the ablation.

Because the native tumor has an ill-defined margin on unenhanced CT images, it is not easy to determine the tumor location.²¹ To resolve this problem, we used nodules that were treated with TACE prior to cryoablation. TACE with lipiodol enables visualization of the HCC nodules as areas in which the lipiodol is deposited. The clear ablation zone of cryoablation can be used to measure the acquired ablative margin^{4,5}. However, cryoablation may lead to deformation of the lipiodol deposition, which influences the assessment of the MAM. In our study, seven of the nine lesions were treated by cryoablation combined with TACE. The MAM was assessed on the fused images of intraoperative CT images, thereby resolving the disadvantage of deformation of the lipiodol deposition during the procedure.

When the tumor is located in the subcapsular region, the potential

advantages of cryoablation relative to RFA include an adequate tumor coverage while avoiding excessively large ablation volumes, or limiting the ablation spread to the adjacent critical structures, and less diaphragmatic injury and post-procedural pain^{3,22,23}. Several factors influence the effect of freezing, including the freezing temperature, freezing time, thawing, and the number of freeze-thaw cycles. The freezing time controls the size of the iceball, which increases with an increase in the freezing time, until a dynamic balance of cold/heat exchange is achieved. As the iceball formation can be visualized with unenhanced CT,²⁴ it can be monitored accurately to ensure complete ablation.⁹ In our study, eight of the nine LTPs occurred in the subcapsular region. For these tumors in our study, the freezing time was tightly controlled in order to avoid complications. The results of the study, therefore, suggest that LTP

Table 1
Patients' characteristics (n = 9).

Patient No.	Age/Sex	Tumor size, mm	Tumor characteristics on unenhanced CT	Segment	Performance status	Subcapsular location	Liver Child-Pugh Classification	Etiology of liver disease	Previous treatment
1	64/M	25.7	Lipiodol deposition + low density	S4	1	Yes	A	Hepatitis B virus	Resection, TACE
2	69/F	32.2	Low density	S7	1	Yes	A	Hepatitis B virus	TACE
3	66/M	31.2	Lipiodol deposition	S2	1	Yes	A	Hepatitis B virus, schistosomiasis	TACE
4	59/M	15.8	Lipiodol deposition + low density	S4	1	Yes	A	Hepatitis B virus	TACE
5	59/F	7.6	Low density	S6	1	No	A	No	Resection
6	53/M	15.8	Low density	S7	1	Yes	A	No	Resection
7	70/M	22.3	Lipiodol deposition + low density	S8	1	Yes	A	Hepatitis B virus	TACE
8	58/M	23.4	Lipiodol deposition + low density	S6	1	Yes	A	Hepatitis B virus	Resection, TACE
9	63/F	30.7	Lipiodol deposition + low density	S6	1	Yes	A	Hepatitis B virus	RFA, TACE

TACE, transcatheter arterial chemoembolization; RFA, radiofrequency ablation.

Table 2
Location of the minimal ablative margin and relationship to the location of local tumor progression.

Lesion	Location of minimal ablative margin ^a						Location of LTP
	Cranial	Caudal	Ventral	Dorsal	Right	Left	
1		+			+		Congruent
2	+			+		+	Congruent
3	+			+			Congruent
4	+					+	Congruent
5		+			+		Congruent
6	+			+	+		Congruent
7	+		+				Congruent
8	+		+			+	Congruent
9		+	+		+		Congruent

^a The location is relative to the original HCC lesion.

occurrence in the subcapsular region of the liver may be a result of an incomplete cryoablation. There is an increasing clinical and experimental evidence that RFA may, in fact, promote off-target tumorigenic effects in incompletely treated tumors at the ablative margin.²⁵ Therefore, it is conceivable that an incomplete cryoablation may induce such off-target tumorigenic effects, resulting in more LTPs. This hypothesis, however, needs further validation.

Although RFA combined with TACE is both safe and feasible for small HCC lesions in special locations, the rate of LTP in these locations is significantly higher than that in non-special locations. The mean time to LTP in the special location group was 14.4 months.²⁶ RFA combined with TACE may maximize the anti-tumor effect. This is important for HCC lesions with a subcapsular location because the peripheral tumor is difficult to completely ablate using RFA; however, RFA after TACE improves the transduction of heat to the peripheral tissues, which reduces the risk for recurrence and metastasis.^{27–29} In our study, the median time to LTP for the seven lesions treated with cryoablation combined with TACE was 7 months (range, 2–35 months). In a previous study, the meantime to LTP after RFA in non-subcapsular HCC was 13.3 ± 9.7 months.¹⁴ However, it remains unknown whether cryoablation combined with TACE may reduce LTP in subcapsular HCCs.

For the fusion image creation, we adopted the automatic rigid registration and manual correction, as previously reported.^{14,15,30–32} After image registration and correction, the post-RFA images were fused to the pre-RFA images. However, the fusion images based on pre- and post-RFA images have some limitations, such as deformation of the liver because of differences in the patient's pose¹⁶ and the variations in slice thickness of the images.¹⁴ These points may influence the precision of the registration and the MAM assessment. Our study used intraoperative unenhanced CT images to create the fused images, which has not been explored in previous studies. Our results showed that the median time

required to fuse the images was 5:17 min (range, 5:04–7:37 min). This is not consistent with the reported results of other studies: the total time required for the creation of fused images was 15.5 ± 5.5 min (range: 8–22 min) in all cases in the study reported by Wang et al.¹⁵ and less than 15 min in all cases in the study reported by Makino et al.¹⁴ These differences in the previous reports might be attributed to the same patient's pose and slice thickness of the intraoperative images of cryoablation seen in our study. The total time required for fusing the images was shorter than that in the aforementioned studies, suggesting feasibility for routine clinical practice.

A previous study showed that the site of LTP was congruent with the area of the MAM in all HCC lesions (31). Concordance between the LTP and the MAM was observed in 83.3% (25/30) of the cases, which was considered as consistent with the findings of a previous study.³² This is also consistent with our results. This is a first report in which this particular technique of fusing images was used for the evaluation of LTP after cryoablation. The advantages of this technique include the simultaneous assessment of the MAM, which reduces the time interval between the treatment and retreatment and thus circumvents the need to perform immediate contrast-enhanced CT or MRI scans.

There were limitations to our study. First, this was a retrospective study with a small number of subjects, thereby resulting in a limited statistical power. Additionally, the correlation between the MAM and the LTP was not assessed because of the limited sample. Second, the spatial resolutions of the reconstructed sagittal and coronal images were too low to accurately evaluate the MAM because the slice thickness of the CT images used to create the fusion images was 3.0 mm. Hence, the evaluation of the tumors' cranial and caudal side may be somewhat inaccurate. Third, lipiodol does not always deposit throughout the nodule. Therefore, it was difficult to determine the exact location of the tumor during the cryoablation procedure.

In conclusion, CT-CT image fusion enables areal-time intraoperative treatment evaluation for visible HCC on unenhanced CT images. Fused imaging evaluation has proved to be an accurate and useful tool for the assessment of cryoablation margins.

Funding

This work was supported by the National Key Research and Development Program of China (No.2016YFC0106203) and the Program of Shanghai Hospital Development Center (No. SHDC22017102).

References

1. Dimitroulis D, Damaskos C, Valsami S, et al. From diagnosis to treatment of hepatocellular carcinoma: an epidemic problem for both developed and developing world. *World J Gastroenterol.* 2017;23:5282–5294.

2. Khemlina G, Ikeda S, Kurzrock R. The biology of Hepatocellular carcinoma: implications for genomic and immune therapies. *Mol Cancer*. 2017;16:149.
3. Wu S, Hou J, Ding Y, et al. Cryoablation versus radiofrequency ablation for hepatic malignancies: a systematic review and literature-based analysis. *Medicine (Baltim)*. 2015;94, e2252.
4. Littrup PJ, Ahmed A, Aoun HD, et al. CT-guided percutaneous cryotherapy of renal masses. *J Vasc Interv Radiol*. 2007;18:383–392.
5. Littrup PJ, Freeman-Gibb L, Andea A, et al. Cryotherapy for breast fibroadenomas. *Radiology*. 2005;234:63–72.
6. Sabel MS. Cryo-immunology: a review of the literature and proposed mechanisms for stimulatory versus suppressive immune responses. *Cryobiology*. 2009;58:1–11.
7. Ladd AP, Rescorla FJ, Baust JG, et al. Cryosurgical effects on growing vessels. *Am Surg*. 1999;65:677–682.
8. Arciero CA, Sigurdson ER. Liver-directed therapies for patients with primary liver cancer and hepatic metastases. *Curr Treat Options Oncol*. 2006;7:399–409.
9. Niu LZ, Li JL, Xu KC. Percutaneous cryoablation for liver cancer. *J Clin Transl Hepatol*. 2014;2:182–188.
10. Goldberg SN, Grassi CJ, Cardella JF, et al. Image-guided tumor ablation: standardization of terminology and reporting criteria. *Radiology*. 2005;235:728–739.
11. Rhim H, Goldberg SN, Dodd GD, et al. Essential techniques for successful radiofrequency thermal ablation of malignant hepatic tumors. *RadioGraphics*. 2001;21 Spec. S17–35; discussion S6–9.
12. Curley SA. Radiofrequency ablation of malignant liver tumors. *Ann Surg Oncol*. 2003;10:338–347.
13. Ahn SJ, Lee JM, Lee DH, et al. Real-time US-CT/MR fusion imaging for percutaneous radiofrequency ablation of hepatocellular carcinoma. *J Hepatol*. 2017;66:347–354.
14. Makino Y, Imai Y, Igura T, et al. Utility of computed tomography fusion imaging for the evaluation of the ablative margin of radiofrequency ablation for hepatocellular carcinoma and the correlation to local tumor progression. *Hepatol Res*. 2013;43:950–958.
15. Wang XL, Li K, Su ZZ, et al. Assessment of radiofrequency ablation margin by MRI-MRI image fusion in hepatocellular carcinoma. *World J Gastroenterol*. 2015;21:5345–5351.
16. Luu HM, Klink C, Niessen W, et al. Non-rigid registration of liver CT images for CT-guided ablation of liver tumors. *PLoS One*. 2016;11, e0161600.
17. Bruix J, Sherman M. Practice guidelines committee AASLD. Management of hepatocellular carcinoma. *Hepatology*. 2005;42:1208–1236.
18. Catalano O, Lobianco R, Esposito M, et al. Hepatocellular carcinoma recurrence after percutaneous ablation therapy: helical CT patterns. *Abdom Imag*. 2001;26:375–383.
19. Goldberg SN, Grassi CJ, Cardella JF, et al. Image-guided tumor ablation: standardization of terminology and reporting criteria. *J Vasc Interv Radiol*. 2009;20: S377–S390.
20. Wang H, Littrup PJ, Duan Y, et al. Thoracic masses treated with percutaneous cryotherapy: initial experience with more than 200 procedures. *Radiology*. 2005;235: 289–298.
21. Koda M, Tokunaga S, Fujise Y, et al. Assessment of ablative margin after radiofrequency ablation for hepatocellular carcinoma; comparison between magnetic resonance imaging with ferucarbotran and enhanced CT with iodized oil deposition. *Eur J Radiol*. 2012;81:1400–1404.
22. Silverman SG, Tuncali K, Adams DF, et al. MR imaging-guided percutaneous cryotherapy of liver tumors: initial experience. *Radiology*. 2000;217:657–664.
23. Tatli S, Acar M, Tuncali K, et al. Percutaneous cryoablation techniques and clinical applications. *Diagn Interv Radiol*. 2010;16:90–95.
24. Lee Jr FT, Chosy SG, Littrup PJ, et al. CT-monitored percutaneous cryoablation in a pig liver model: pilot study. *Radiology*. 1999;211:687–692.
25. Ahmed M, Kumar G, Moussa M, et al. Hepatic radiofrequency ablation-induced stimulation of distant tumor growth is suppressed by c-met inhibition. *Radiology*. 2016;279:103–117.
26. Guo YJ, Huang WS, Zhou B, et al. Transarterial chemoembolization plus computed tomography-guided percutaneous radiofrequency ablation for small hepatocellular carcinoma in special locations. *Zhonghua Yixue Zazhi*. 2013;93:2627–2630.
27. Wang ZJ, Wang MQ, Duan F, et al. Transcatheter arterial chemoembolization followed by immediate radiofrequency ablation for large solitary hepatocellular carcinomas. *World J Gastroenterol*. 2013;19:4192–4199.
28. Yuan H, Liu F, Li X, et al. Angio-CT-guided transarterial chemoembolization immediately in combination with radiofrequency ablation for large hepatocellular carcinoma. *Acad Radiol*. 2019;26:224–231.
29. Yuan H, Liu F, Li X, et al. Transcatheter arterial chemoembolization combined with simultaneous DynaCT-guided radiofrequency ablation in the treatment of solitary large hepatocellular carcinoma. *Radiol Med*. 2019;124:1–7.
30. Makino Y, Imai Y, Igura T, et al. Comparative evaluation of three-dimensional Gd-EOB-DTPA-enhanced MR fusion imaging with CT fusion imaging in the assessment of treatment effect of radiofrequency ablation of hepatocellular carcinoma. *Abdom Imag*. 2015;40:102–111.
31. Tomonari A, Tsuji K, Yamazaki H, et al. Feasibility of fused imaging for the evaluation of radiofrequency ablative margin for hepatocellular carcinoma. *Hepatol Res*. 2013;43:728–734.
32. Kim YS, Lee WJ, Rhim H, et al. The minimal ablative margin of radiofrequency ablation of hepatocellular carcinoma (> 2 and < 5 cm) needed to prevent local tumor progression: 3D quantitative assessment using CT image fusion. *AJR Am J Roentgenol*. 2010;195:758–765.